

Selective separation of manganese, cobalt and nickel in a fully aqueous system

Nicolas Schaeffer,^[a] Helena Passos,^[a] Matthieu Gras,^[b] Sílvia Juliana Rodriguez Vargas,^[a] Márcia C. Neves,^[a] Lenka Svecova,^[b] Nicolas Papaiconomou^[c] and João A.P. Coutinho*^[a]

^[a] *CICECO, Aveiro Institute of Materials, Department of Chemistry, University of Aveiro, Campus Universitário de Santiago, 3810-193 Aveiro, Portugal.*

^[b] *Univ. Grenoble Alpes, Univ. Savoie Mont Blanc, CNRS, Grenoble INP, LEPMI, 38000 Grenoble, France.*

^[c] *Université Nice Sophia Antipolis, Department of Chemistry, 28 Avenue Valrose, 06103 Nice, France*

* Corresponding authors: jcoutinho@ua.pt

Number of pages: 13

Number of Figures: 9

Number of Tables: 3

METHODOLOGY

Materials and Methods

Metal concentration was determined by atomic adsorption spectroscopy (AAS) using a PinAAcle 900F (Perkin Elmer) spectrometer. ^1H -, ^{12}C - and ^{31}P -NMR spectroscopy of $[\text{P}_{44414}]\text{Cl}$ solutions were recorded using a 300 MHz Bruker Avance III spectrometer with D_2O as solvent. $[\text{P}_{44414}]^+$ concentration in the was determined by quantitative ^1H -NMR with benzene as internal standard. Water content of the IL-rich phase was determined using an 831 KF Coulometer (Metrohm). Sample morphology was analysed by scanning electron microscopy (SEM) with energy-dispersive X-ray spectroscopy (EDS) using a Bruker Nano GmbH microscope after carbon sputter-coating. Fourier transform infrared (FTIR) spectra were recorded on a Galaxy Series 7000 spectrometer equipped with an attenuated total reflectance (ATR) accessory (Golden Gate). Temperature controlled UV-vis spectra were recorded on a Shimadzu UV-1800 spectrophotometer fitted with a TCC-100 Thermoelectrically cell holder (accuracy of ± 0.1 °C). Dynamic Light Scattering (DLS) measurements (Malvern Zetasizer Nano-ZS) were carried out to evaluate the change in aggregate size with temperature. Samples were irradiated with red light (a HeNe laser, a wavelength of 665 nm) and the intensity fluctuations of the scattered light were detected at a backscattering angle of 173° to generate an autocorrelation function. The cumulant analysis of this function provided by software DTS v 7.03 yielded the particle size and the distribution width. All studied system compositions were determined by the weight quantification of all components added within an uncertainty of $\pm 10^{-3}$ g using a Mettler Toledo XP205 analytic balance.

The IL tributyltetradecyl phosphonium chloride ($[\text{P}_{44414}]\text{Cl}$) was purchased from Iolitec in 95 wt.% purity and confirmed as 97.1 wt.% pure by quantitative ^1H -NMR analysis. Cobalt chloride hexahydrate (99% purity) and manganese chloride tetrahydrate (99% purity) were obtained from Merck and nickel chloride hexahydrate (97% purity) was acquired from BDH Chemicals. Hydrochloric acid (37%) was obtained from Fisher Scientific and anhydrous sodium carbonate (99.9% purity) from Prolabo. Ultrapure, double distilled water passed through a reverse osmosis system and further treated with a Milli-Q plus 185 water purification apparatus (18.2 m Ω at 298 K) was used for all experiments.

Calibration of ozone generator

A commercially available domestic ozone generator (LufthousO₃ from Lufthous) was used in all experiments delivering a fixed gas flow rate of 1.0 L.min⁻¹ monitored using a flow meter. The ozone flow rate was determined by colorimetric titration using potassium iodide and sodium thiosulfate ($\text{Na}_2\text{S}_2\text{O}_3$). Firstly, in a cylindrical vessel of diameter 5 cm and height 30 cm, ozone was bubbled through a 100 mL

solution of KI of known molarity for a determined time resulting in an intense orange coloured final solution according to the reaction:



Secondly, after 10 min of oxidation the obtained orange solution was titrated using a $\text{Na}_2\text{S}_2\text{O}_3$ solution of known molarity until colourless according to the reaction:



This procedure was repeated twice and a consistent ozone flow rate of 0.768 g.hr^{-1} ($0.016 \text{ mol.hr}^{-1}$) was obtained.

Determination of $\text{MCl}_2\text{-[P}_{44414}\text{]Cl-H}_2\text{O}$ phase diagram and cobalt speciation with temperature

The procedure followed in this work for the experimental determination of binodal curves for ternary and quaternary systems was previously reported.¹ The binodal curves of the $\text{NiCl}_2\text{-[P}_{44414}\text{]Cl-H}_2\text{O}$ ternary system and $\text{NiCl}_2\text{-[P}_{44414}\text{]Cl-HCl-H}_2\text{O}$ quaternary system at $25.0 \text{ }^\circ\text{C}$ and/or $50.0 \text{ }^\circ\text{C}$ were determined by the cloud point titration method in a temperature-controlled cell under agitation and atmospheric pressure. Starting aqueous solutions of $[\text{P}_{44414}\text{]Cl}$ (70.0 wt%) and saturated solutions of chloride salts were prepared and used for the determination of the binodal curves. The phase diagrams for the quaternary $\text{NiCl}_2\text{-[P}_{44414}\text{]Cl-HCl-H}_2\text{O}$ system containing a fixed HCl concentration (3.7 wt %) was obtained by maintaining a constant 3.7 wt.% HCl concentration in all solutions used throughout the cloud point titration procedure. The ternary and quaternary system compositions were determined by the weight quantification of all components added within an uncertainty of $\pm 10^{-3} \text{ g}$.

REFERENCES

[1] Neves, C.M.S.S.; Ventura, S.P.M.; Freire, M.G.; Marrucho, I.M.; Coutinho, J.A.P. Evaluation of Cation Influence on the Formation and Extraction Capability of Ionic-Liquid-Based Aqueous Biphasic Systems. *J. Phys. Chem. B*, **2009**, 113, 5194–5199.

FIGURES

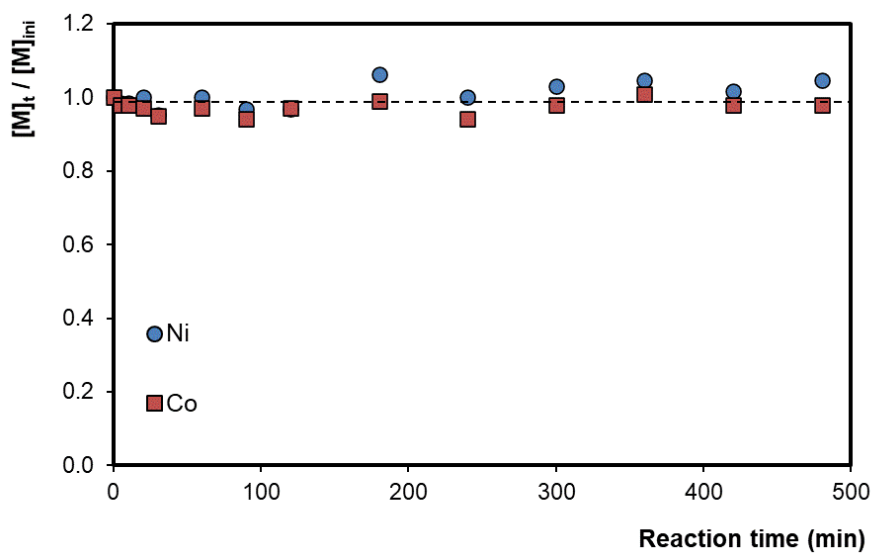


Figure S1. Evolution of the cobalt and nickel concentration with time during the continued ozonation of manganese in aqueous solution. The concentration of cobalt and nickel are standardized according to their initial concentration (Mn:Co:Ni molar ratio of 0.07:0.17:1.00 and $[\text{NiCl}_2 \cdot 6\text{H}_2\text{O}]_{ini} = 0.32 \text{ mol.kg}^{-1}$).

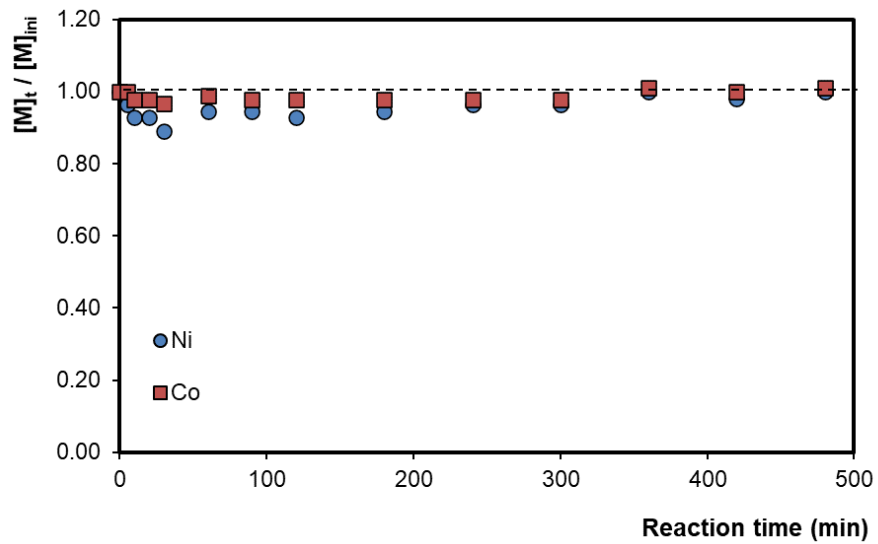


Figure S2. Evolution of the cobalt and nickel concentration with time during the continued ozonation of manganese in 3.7 wt.% HCl solution. The concentration of cobalt and nickel are standardized according to their initial concentration (Mn:Co:Ni molar ratio of 0.07:0.17:1.00 and $[\text{NiCl}_2 \cdot 6\text{H}_2\text{O}]_{\text{ini}} = 0.32 \text{ mol} \cdot \text{kg}^{-1}$).

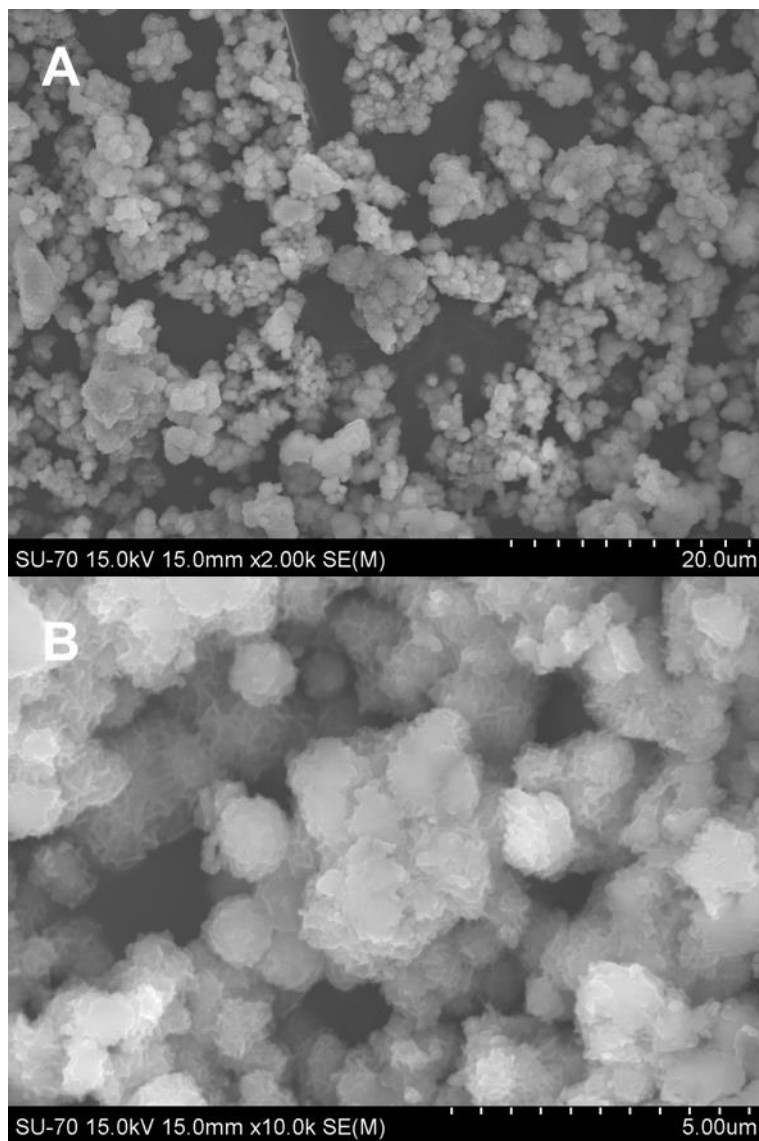


Figure S3. SEM image of the precipitate recovered after 480 min ozonation from neutral aqueous solution under A) low and B) high magnification.

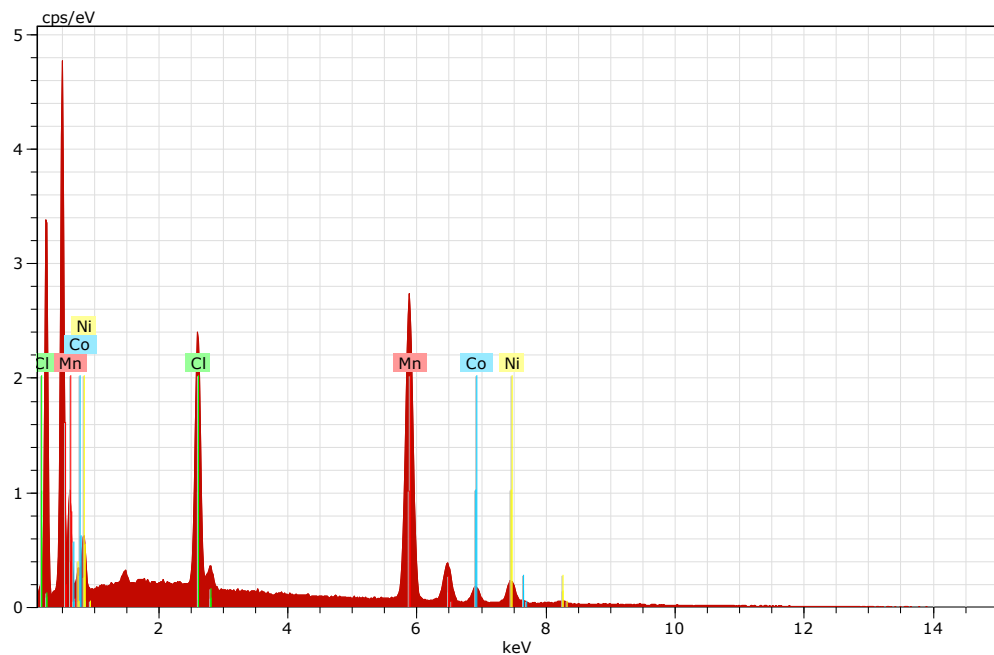


Figure S4. Energy dispersive X-ray analysis of the precipitate in **Figure S3** recovered after 480 min from an aqueous solution.

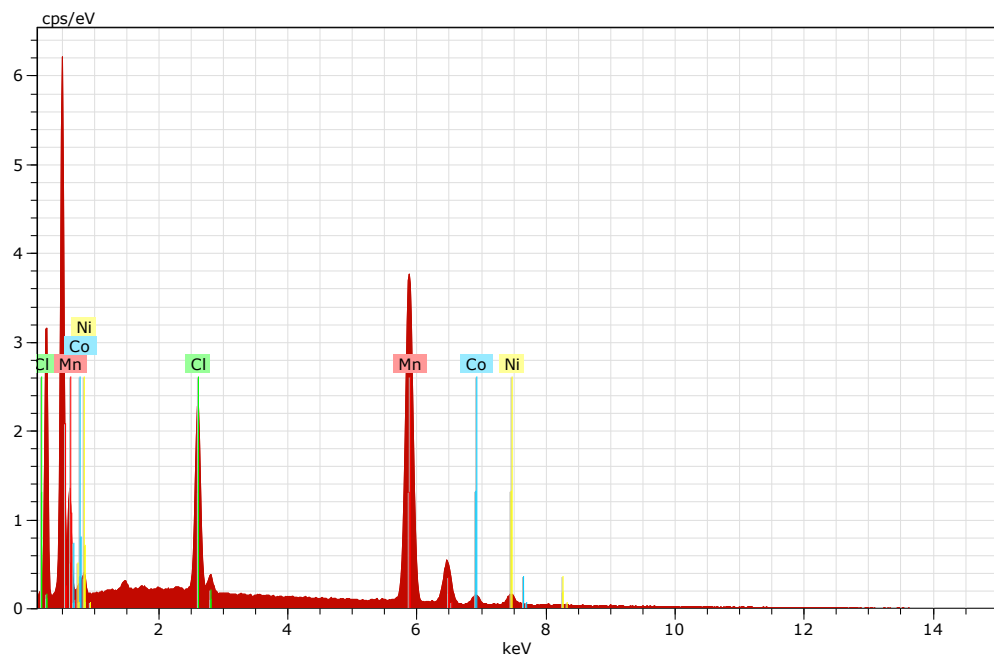


Figure S5. Energy dispersive X-ray analysis of the precipitate in **Figure 2** of the manuscript recovered after 480 min from a 3.7 wt.% HCl solution.

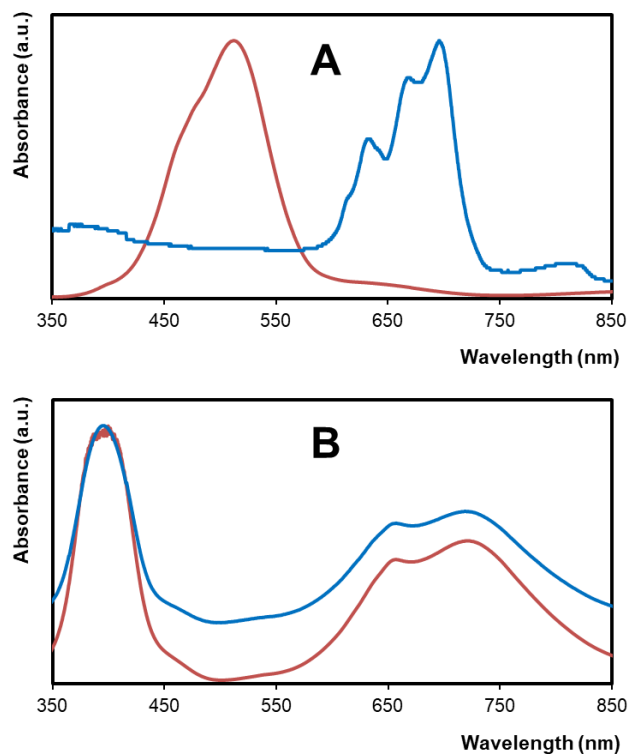


Figure S6. UV-vis spectra of the IL-rich (blue) and salt-rich (red) phases in the A) CoCl_2 -[P_{44414}]Cl- H_2O ABS and B) the NiCl_2 -[P_{44414}]Cl- H_2O at $T=50.0\text{ }^\circ\text{C}$ ($[\text{P}_{44414}]\text{Cl}=30.0\text{ wt.}\%$, $[\text{NiCl}_2]=[\text{CoCl}_2]=10.0\text{ wt.}\%$).

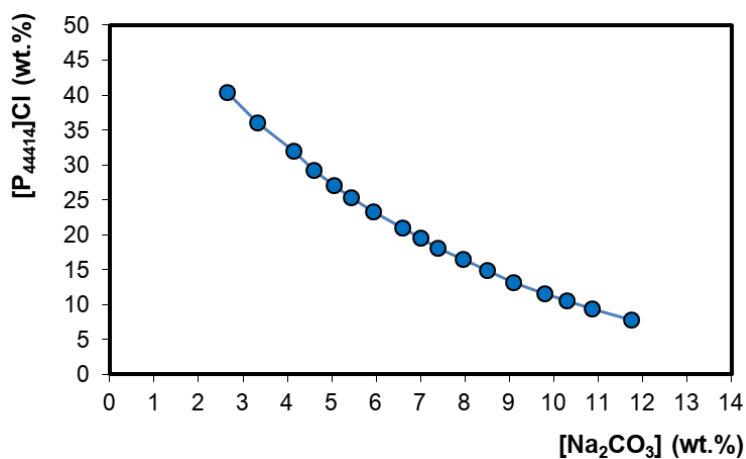


Figure S7. Binodal curve of the Na_2CO_3 -[P_{4444}]Cl- H_2O ABS at $25.0\text{ }^\circ\text{C}$.

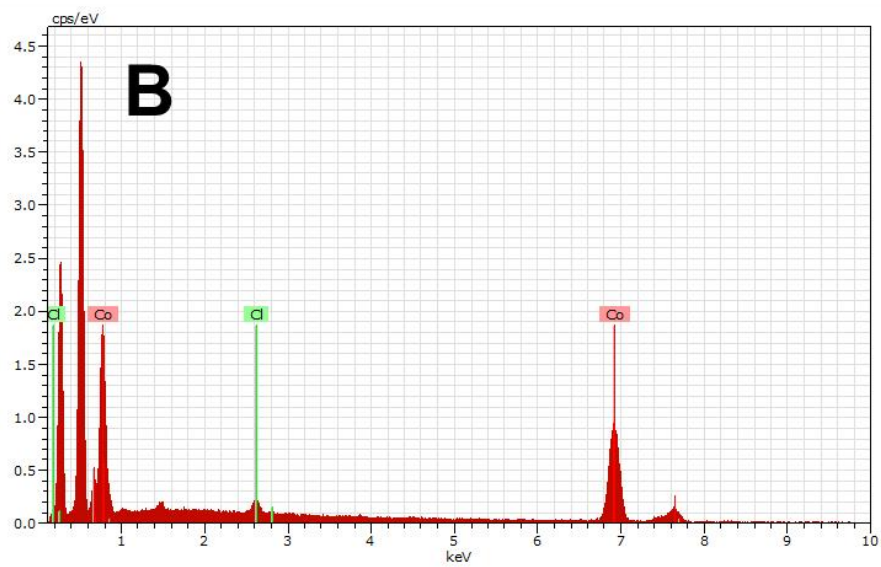
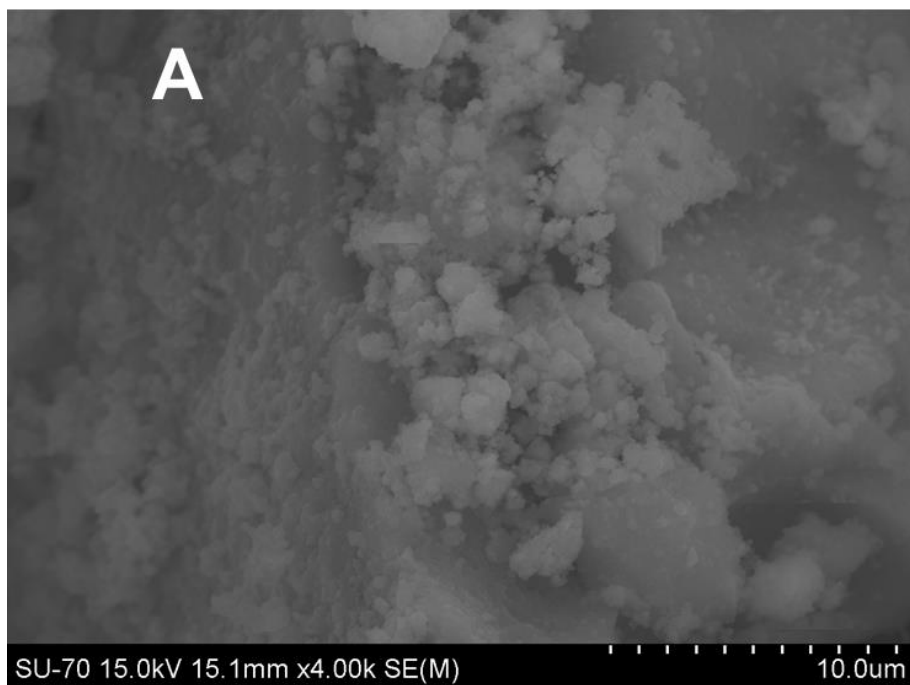


Figure S8. A) SEM image and B) Energy dispersive X-ray analysis of the recovered precipitate obtained after 8x dilution of isolated IL phase and subsequent addition of 1.2 stoichiometric amount Na_2CO_3 (extraction conditions - $\chi_{\text{Co/Ni}} = 0.20$, $[\text{P}_{44414}]\text{Cl} = 20.0$ wt.% and $[\text{NiCl}_2 \cdot 6\text{H}_2\text{O}] = 1.00$ mol.kg⁻¹).

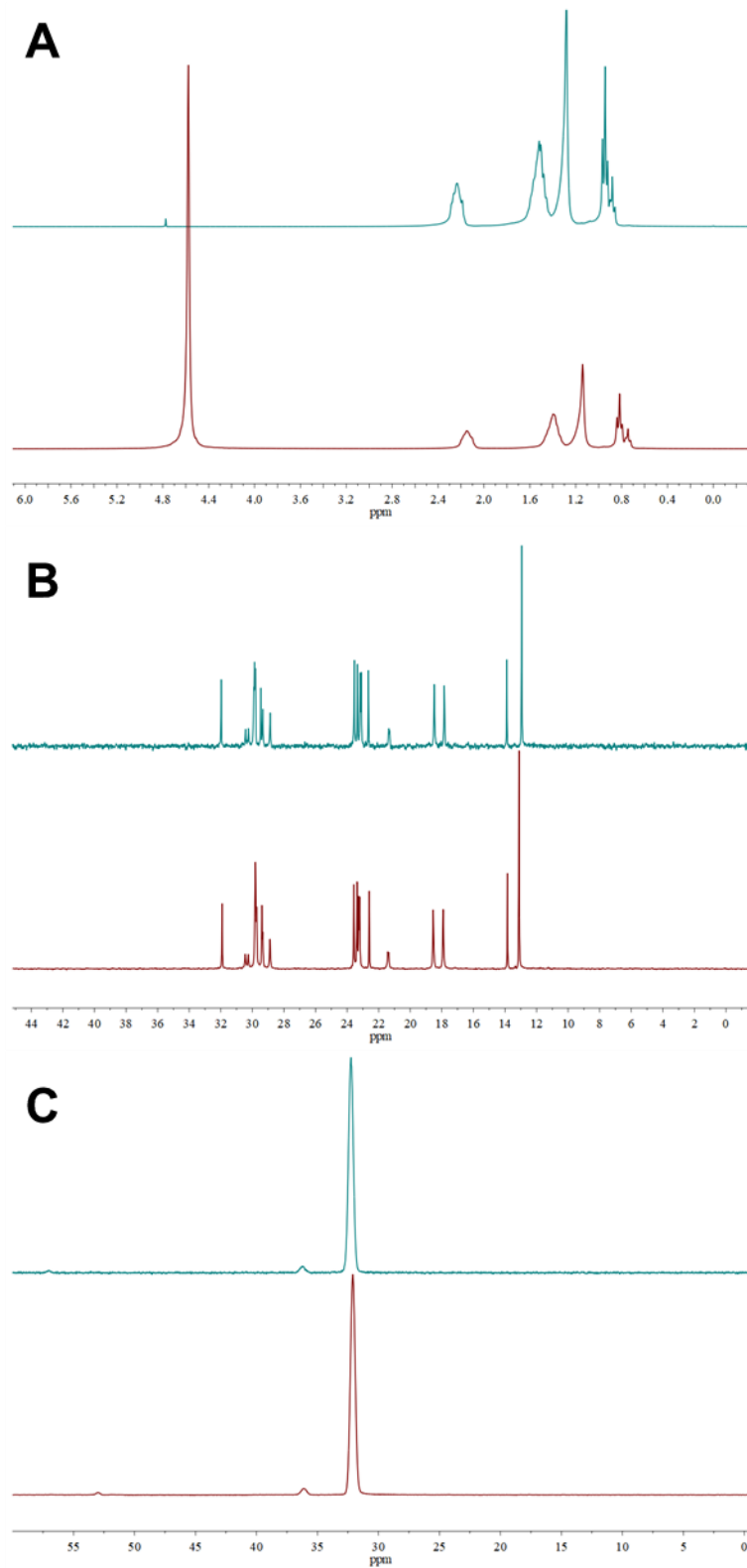


Figure S9. A) 1H -NMR, B) ^{12}C -NMR, and C) ^{31}P -NMR spectra of virgin (blue) and recovered (red) $[P_{44414}]Cl$ (solvent - D_2O).

TABLES

Table S1. Experimental binodal data for the ternary and quaternary systems reported in this work.

25.0 °C		50.0 °C		50.0 °C + 3.7wt.% HCl		25.0 °C	
[NiCl ₂]	[P ₄₄₄₁₄]Cl	[NiCl ₂]	[P ₄₄₄₁₄]Cl	[NiCl ₂]	[P ₄₄₄₁₄]Cl	[Na ₂ CO ₃]	[P ₄₄₄₁₄]Cl
6.51	71.02	2.47	56.80	0.93	56.71	2.64	40.33
7.63	64.04	2.55	46.91	0.93	53.17	3.32	36.00
7.75	60.06	2.55	45.12	0.94	49.51	4.15	31.92
8.35	57.62	2.57	43.67	0.95	45.75	4.59	29.17
8.46	55.51	2.64	42.39	0.94	42.65	5.06	27.08
8.99	51.67	2.69	40.82	1.01	38.63	5.44	25.32
9.63	48.12	2.74	39.81	1.02	35.04	5.93	23.35
9.86	46.62	2.77	38.73	1.04	32.20	6.59	20.95
10.26	44.92	2.86	37.62	1.11	28.10	7.00	19.49
10.80	40.76	2.88	36.74	1.10	24.10	7.39	18.15
11.58	36.80	2.91	35.60	1.16	21.32	7.96	16.49
11.71	35.90	2.94	34.85	1.24	19.47	8.51	14.87
11.96	34.25	2.99	33.95	1.25	18.63	9.10	13.24
12.05	33.01	3.05	32.88	1.29	17.52	9.80	11.58
12.17	32.25	3.04	31.73	1.33	16.50	10.29	10.50
12.22	31.62	3.14	30.96	1.39	15.72	10.86	9.35
12.45	30.72	3.21	30.04	1.46	14.52	11.76	7.76
12.57	29.57	3.29	29.02	1.51	13.58		
12.90	28.12	3.29	28.37	1.58	12.85		
13.13	26.88	3.40	27.19	1.64	11.95		
13.37	25.80	3.42	26.40	1.71	11.16		
13.43	25.01	3.47	25.64	1.78	10.49		
13.49	24.19	3.50	24.85	1.87	9.56		
13.76	23.16	3.63	23.81	1.91	9.05		
13.80	22.53	3.68	22.76	2.04	8.17		
14.00	21.51	3.76	21.90	2.06	7.63		
14.27	20.18	3.82	21.05	2.09	7.28		
14.31	19.31	3.86	20.36	2.18	6.80		
14.34	18.87	3.93	19.63	2.20	6.62		
14.43	18.38	3.98	19.03	2.25	6.22		
14.49	17.92	4.13	17.94	2.40	5.12		
14.60	17.38	4.23	17.09				
14.80	16.49	4.36	16.54				
14.92	15.73	4.35	15.79				
15.04	15.03	4.46	14.65				

15.10	14.34	4.56	14.08
15.29	13.67	4.74	12.57
15.37	12.88	5.14	9.65
15.54	12.15	5.31	8.40
15.58	11.70	5.54	6.18
15.65	11.24	5.81	4.51
15.74	10.82		
15.85	10.45		
15.89	10.12		
15.93	9.88		
16.04	9.58		
16.07	9.32		
16.10	9.07		
16.19	8.79		
16.21	8.71		
16.18	8.63		
16.22	8.50		
16.26	8.38		
16.28	8.28		
16.35	8.10		
17.09	4.60		

Table S2. Cobalt and nickel distribution coefficients (D_M) as a function of the cobalt:nickel molar ratio ($\chi_{Co/Ni}$) presented in **Figure 5A**. Distribution coefficients and cobalt-nickel separation factor ($\alpha_{Co/Ni}$) are the average value from three separate measurements. Extraction conditions - $[P_{44414}]Cl= 20.0$ wt.%, $[NiCl_2 \cdot 6H_2O]= 0.35$ mol.kg⁻¹, $[HCl] = 1.00$ mol. kg⁻¹.

$\chi_{Co/Ni}$	D_{Ni}		D_{Co}		$\alpha_{Co/Ni}$	
	Average	STD	Average	STD	Average	STD
0.00	0.21	0.02	0.00	0.00	0.00	0.00
0.05	0.20	0.01	0.47	0.11	2.36	0.71
0.10	0.16	0.01	0.62	0.13	3.98	0.94
0.15	0.15	0.01	0.75	0.11	5.07	0.75
0.20	0.12	0.01	0.79	0.03	6.72	0.59
0.25	0.12	0.01	0.96	0.04	8.36	0.93
0.33	0.10	0.02	1.43	0.04	14.9	2.74

Table S3. Cobalt and nickel distribution coefficients (D_M) as a function of the cobalt:nickel molar ratio ($\chi_{Co/Ni}$) presented in **Figure 5B**. Distribution coefficients and cobalt-nickel separation factor ($\alpha_{Co/Ni}$) are the average value from three separate measurements. Extraction conditions - $[P_{44414}]Cl= 20.0$ wt.%, $[NiCl_2 \cdot 6H_2O]= 1.00$ mol.kg⁻¹, $[HCl] = 0.00$ mol. kg⁻¹.

$\chi_{Co/Ni}$	D_{Ni}		D_{Co}		$\alpha_{Co/Ni}$	
	Average	STD	Average	STD	Average	STD
0.00	0.10	0.01	0.00	0.00	0.00	0.00
0.05	0.09	0.02	3.23	0.08	39.1	11.8
0.10	0.07	0.02	4.45	0.11	71.3	21.8
0.15	0.06	>0.01	6.29	0.29	114.9	10.4
0.20	0.03	0.01	12.2	1.50	483.9	77.7
0.25	0.02	>0.01	5.28	0.67	366.4	122.8
0.33	0.01	>0.01	3.17	0.37	292.3	92.0